
Optimization Landscapes Learned: Proxy Networks Boost Convergence in Physics-based Inverse Problems

Girnar Goyal¹, Philipp Holl², Sweta Agrawal³, Nils Thuerey²

¹Ludwig Maximilian University of Munich,

²Technical University of Munich, ³Instituto de Telecomunicações

girigoyal@gmail.com

Abstract

Solving inverse problems in physics is central to understanding complex systems and advancing technologies in various fields. Iterative optimization algorithms, commonly used to solve these problems, often encounter local minima, chaos, or regions with zero gradients. This is due to their overreliance on local information and highly chaotic inverse loss landscapes governed by underlying partial differential equations (PDEs). In this work, we show that deep neural networks successfully replicate such complex loss landscapes through spatio-temporal trajectory inputs. They also offer the potential to control the underlying complexity of these chaotic loss landscapes during training through various regularization methods. We show that optimizing on network-smoothened loss landscapes leads to improved convergence in predicting optimum inverse parameters over conventional momentum-based optimizers such as BFGS on multiple challenging problems.

1 Introduction

Solving inverse problems is pivotal across scientific and engineering domains, with applications ranging from optimizing fluid dynamics (Oulghelou et al., 2022) and materials design (Fung et al., 2021) to enhancing structural health monitoring (McCann et al., 2017), manufacturing optimization (Würth et al., 2023), and weather prediction (Huang et al., 2005). Often, they are difficult to solve as they involve determining the causes of observed effects, and even minor perturbations in the output values can cause significant variations in the reconstructed input. This is why solving inverse problems is a substantially more challenging task than observing the effects themselves in a forward problem.

Various techniques, such as Bayesian inference (Shahriari et al., 2015), quasi-Newton (Ruder, 2017; Broyden et al., 1970), and machine learning methods (Chouzenoux et al., 2021; Cao et al., 2022; Mohammad-Djafari, 2021; Antil et al., 2023), have been devised to solve the inverse problems. Popular iterative methods based on approximations of the Hessian matrix, such as the BFGS (Broyden et al., 1970), often encounter convergence issues in local optima, flat, and chaotic regions of the underlying non-linear inverse loss landscapes. While the local optima attract the optimizers, flat and chaotic regions frequently create directional traps which makes these loss landscapes extremely difficult to optimize. Step size adjustments and the addition of momentum do not fully overcome these challenges.

Recent research investigates using deep neural networks (DNN) as surrogates for the inverse problem governed by non-linear partial differential equations (PDEs), aiming to recover the simulation inputs through end-to-end predictions (Pfrommer et al., 2018; Ren et al., 2021). However, using DNNs for complex inverse problems is challenging due to: (i) limited and noisy data creating the risk of overfitting during training (ii) a lack of understanding of the network learning mechanism (Buhrmester et al., 2021), and (iii) a lack of generalization across inverse problems (Goodfellow et al., 2016).

We instead hypothesize that, when provided with a true spatio-temporal trajectory for which the inverse solutions are sought, a *proxy neural network* (ProxyNN) can be directly trained to predict the **configuration loss** that measures the deviation of this trajectory from that induced by randomly sampled target parameters from the same initial state. However, the non-linearity of these configuration loss landscapes would still remain the core issue in finding optimum solutions to the inverse problems. With our work, we aim to answer the following research questions:

Can we use deep neural networks to model and predict the target configuration loss landscapes? How can we utilize the training process of ProxyNNs to simplify the complexity of the target configuration loss landscapes?

Motivated by the work of Dherin et al. (2022) who utilize regularization methods for controlling the network's complexity during training, we aim to gain control over the underlying complexity of the configuration loss landscapes via several regularization techniques.

We show that ProxyNNs can successfully predict chaotic, non-linear loss landscapes in inverse problems and present the opportunity to steer the underlying complexity during training through various regularization techniques. Under regularization pressure, ProxyNNs learn to predict simpler solutions to such complex landscapes while preserving the fundamental characteristics of the underlying PDEs. We find that optimizing configuration loss landscapes predicted by complexity-controlled ProxyNNs yield better convergence through momentum-based optimizers such as BFGS. We show the improvement in accuracy of the proposed ProxyNN-based optimization over traditional methods in three complex inverse problems: (i) the Inviscid Burgerséquation, representing fluid flow dynamics; (ii) a chaotic system following the Kuramoto-Sivashinsky equation; and (iii) a rigid body N-dimensional simulation inspired by Billiards.

2 Method

Several studies have emphasized the potential of DNNs as effective surrogates for numerical solvers (Würth et al., 2023; Guo et al., 2016; Dias Ribeiro et al., 2020; Wolf et al., 2020; Pfrommer et al., 2018; Nabian & Meidani, 2018; Michoski et al., 2020; Anantha Padmanabha & Zabaras, 2021; Shen et al., 2022). In this work, we demonstrate that the surrogate capabilities of neural networks can be further expanded to approximate intricate relationships between the system trajectory and predicted trajectories evolved through randomly sampled control parameters. We begin by formulating a generalized inverse problem framework where we have access to the spatio-temporal evolution of a physical system, and we aim to recover the influencing control parameters.

2.1 Generalized Landscape for Inverse Problems

In the forward problem, the evolution of an initial physical state Y_0 under the influence of control parameters X^* is obtained by numerically solving the underlying partial differential equation \mathcal{P} as:

$$Y^* = \mathcal{P}(Y_0, X^*)$$

In an inverse problem, our goal is to determine the unknown control parameters X^* from the known trajectory of states Y^* . The key is to quantify how these control parameters influence the spatio-temporal evolution of physical states through underlying physical laws and constraints. This can be done by comparing the trajectory evolved under random values of control parameters $X_s \in Z$, from the initial state Y_0 : $Y_s = \mathcal{P}(Y_0, X_s)$. Both the *true trajectory* (Y^*) and the *comparison trajectory* (Y_s) are numerically computed with the same initial state Y_0 but different control parameters X^* and X_s respectively. To quantify the influence of the control parameters, we define the *Configuration Loss* function as:

$$\mathcal{L}(Y^*, X_s) = \|\mathcal{P}(Y_0, X_s) - Y^*\|_2^2 \quad (1)$$

Optimization of the *Configuration Loss* function in the control parameter space ($X_s \in Z$) would theoretically yield the solution to the inverse problem:

$$X^* = \min_{X_s \in Z} (\mathcal{L}(Y^*, X_s)) \quad (2)$$

In this framework, we expect the configuration loss landscape to obtain a global minimum at the true parameter set value, i.e. $\mathcal{L}(Y^*, X_s)|_{X_s=X^*} = 0$. Depending on the complexity of the physical system and underlying PDEs, the landscape can be geometrically chaotic with multiple local minima and regions of sharp and vanishing gradients. These issues encountered during the optimization of such loss landscapes can be also understood through a popular test case, the Gramacy & Lee function, $f(x) = \frac{\sin(10\pi x)}{2x} + (x-1)^4$ (Gramacy & Lee, 2010). It contains multiple local minima along with a global minimum at $(X_s = 0.143)$ in $[-1, 3]$ (See Figure 1). The local-minima problem causes poor convergence in iterative momentum-based optimizers such as BFGS. Depending on the initial guess of the control parameters, BFGS often yields a piece-wise convergence and fails to converge to the optimum parameters.

In this work, we propose to first replicate the configuration loss landscape, $\mathcal{L}(Y^*, X_s)$, via DNNs which are established as universal function approximators (Section 2.2). However, this would still require finding the global minimum using the model-predicted loss. To sidestep this, we instead aim to gain control over the complexity of the inverse configuration loss landscape during the training of a proxy network via implicit and explicit regularization techniques (Section 2.3) motivated by the work in Dherin et al. (2022).

2.2 ProxyNNs for the “Configuration Loss” Function

The complex geometric features in the *Configuration Loss* landscape motivate the exploration of using machine learning methods. We employ Convolutional Neural Networks (CNN) (Winovich et al., 2019) to train deep proxy neural networks, anticipating that the network can effectively grasp the inherent partial differential equation (PDE) and accurately emulate the configuration loss, (\mathcal{L}) .

For a physical system with a trajectory of states, Y^* , governed by PDE, \mathcal{P} , ProxyNN is trained to map unrelated inputs, Y^* and randomly sampled $X_s \in Z$, to the target configuration loss \mathcal{L} . The network is then trained by minimizing the network training L2 loss, \mathcal{L}_N using the Adam optimizer (Kingma & Ba, 2017) in each step as:

$$\mathcal{L}_N = \|f_\theta(Y^*, X_s) - \mathcal{L}(Y^*, X_s)\|^2 \quad (3)$$

where $\mathcal{L}(Y^*, X_s)$ and $f_\theta(Y^*, X_s)$ represent the ground truth (equation 1) and proxy network predicted configuration loss values for the true trajectory Y^* .

2.3 Modulating ProxyNN’s Complexity through Regularization

This section outlines our approach for controlling the intricacies of learning the landscape of inverse configuration loss. We achieve this by employing a range of implicit and explicit regularization techniques throughout the training of the ProxyNN.

Noise regularization: The networks are trained to replicate the configuration loss function through noise-labeled inputs $(X_s + \sigma \mathcal{N})$ where σ is the scaling hyperparameter for the noise sampled from a Gaussian distribution \mathcal{N} (Blanc et al., 2020; Dherin et al., 2022). The introduction of scaled Gaussian noise puts regularization pressure on the network learning process, which enhances the generalizing capacity of networks and helps mitigate the impact of high-frequency signals within the target configuration loss function.

Loss penalty-based regularization: We observe that the high-frequency geometric features and regions containing maxima or minima are identified at later training stages of the network. Hence, we introduce a training-loss penalty that creates a geometric-bias-based regularization

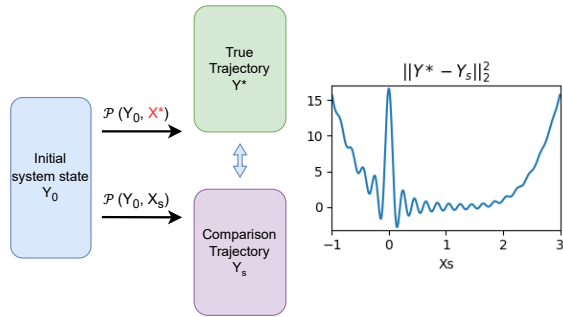


Figure 1: Schematic representation of formulating the *configuration loss* landscape $\mathcal{L} = \|Y_s - Y^*\|^2$. The Gramacy and Lee function represent a test case for configuration loss landscapes in this figure.

during the network training, favoring low-lying regions of the target configuration loss landscape. The network training loss (equation 3) is scaled with the loss-penalty hyperparameter $\mu > 1 : \forall (X_s \in Z)$ where $f_\theta(Y^*, X_s) > \mathcal{L}$. This imposes a regularization influence to encourage improved learning of geometric features near regions that contain minima.

The regularization techniques with hyperparameters $\{\sigma, \mu\}$ can be used to achieve reasonable control over the ProxyNN's complexity with the modified network training loss as:

$$\mathcal{L}_N^R = \mu \times \|f_\theta(Y^*, X_s + \sigma \mathcal{N}) - \mathcal{L}(Y^*, X_s)\|_2^2 \quad (4)$$

The full algorithm to train ProxyNNs is shown below:

Algorithm 1: Training ProxyNNs for Inverse Problems

Input: Ground truth forward simulated trajectories with their true inverse values, $D = \{Y^*, X^*\}_{i=1}^N$, Numerical simulation framework for the underlying PDE, \mathcal{P}

- 1 **for** training step $t = 1 \dots T$ **do**
- 2 Sample state trajectory Y^* from dataset D and extract its initial state Y_0
- 3 **for** i in $1 \dots n$ **do**
- 4 Randomly sample control parameters, $X_s \in Z$
- 5 From Y_0 , simulate comparison trajectory Y_s evolved under X_s , i.e., $Y_s = \mathcal{P}(Y_0, X_s)$
- 6 Compute the true configuration loss between the *true trajectory* and *comparison trajectory*, $\mathcal{L} = \|Y^* - Y_s\|^2$
- 7 Compute ProxyNN predicted configuration loss, $f_\theta(Y^*, X_s)$
- 8 Update ProxyNN parameters using the regularized network training loss, \mathcal{L}_N^R from eq. 4
- 9 **Return** f_θ .

2.4 Optimization Scheme

In general, optimization algorithms based on Newton's methods exhibit rapid convergence but face challenges, such as the computationally expensive calculation of the inverse Hessian matrix and potential numerical instabilities with poorly conditioned Hessians. Quasi-Newton second-order algorithms, like the Broyden–Fletcher–Goldfarb–Shanno algorithm (BFGS), address these issues by approximating the Hessian matrix using information from first-order gradients, requiring less computational cost per iteration. However, they encounter limitations in landscapes with non-linearity, struggling to reach global minima and being susceptible to local minima or saddle points.

To improve convergence in a given non-linear inverse problem, we formulate a two-step optimization strategy utilizing the ProxyNNs trained with regularization hyperparameters $\{\sigma, \mu\}$ (see section B). In the primary optimization step, we employ BFGS on the configuration loss landscape predicted by the regularized ProxyNNs. The underlying regularization effect is expected to lead to convergence near the global minimum, avoiding regions with local minima and steep gradients in the target landscape. To ensure that the predictions can potentially reach arbitrarily high levels of accuracy, a secondary BFGS optimization is introduced. We treat the outcome of the primary step convergence as an initial guess for the secondary step, conducted on the ground truth configuration loss function (\mathcal{L}). The goal in this step is to attain the optimal solution X^* within the *region of interest*, i.e., the vicinity of the global minimum.

3 Experimental Setup

We perform a series of numerical experiments to investigate (i) the capabilities of ProxyNNs to replicate and regularize the configuration loss function \mathcal{L} and (ii) the optimization performance of regularized ProxyNNs benchmarked against existing iterative methods.

3.1 Non-Linear Inverse Problems

We evaluate our methodology for the following non-linear physical systems: **Burgers' equation**: The inviscid Burgers' equation (Burgers, 1948; Hopf, 1950) is a fundamental nonlinear first-order

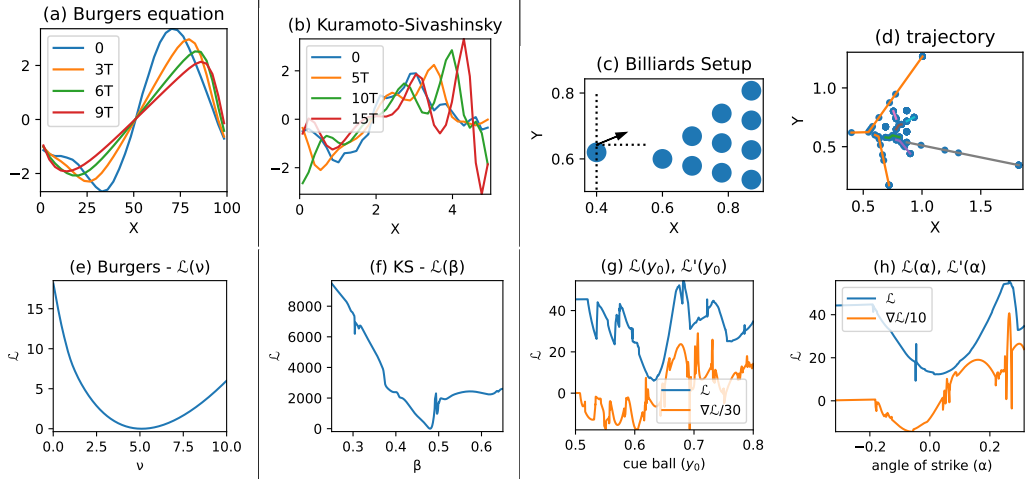


Figure 2: System trajectories and *configuration loss* landscapes (\mathcal{L}) for non-linear inverse problems in (a,e) Burgers equation, (b,f) for the Kuramoto-Sivashinsky equation, and (c,d) and (g,h) for the Billiards-2D setup respectively. These landscapes (f-h) encounter convergence issues in iterative optimizers due to local minima and regions of sharp and vanishing gradients.

hyperbolic partial differential equation that describes the dynamics of a fluid flow and is used in various fields to model a wide range of phenomena (Savović et al., 2023). The velocity field can exhibit interesting behavior such as the formation of shock waves and turbulence. The equation is written as:

$$\frac{\partial u}{\partial t} + u \frac{\partial u}{\partial x} = \nu \frac{\partial^2 u}{\partial x^2}$$

where $u(x, t)$ is the velocity field, and ν is the kinematic viscosity or diffusivity of the fluid system, which we aim to recover through the solution of the inverse problem.

Kuramoto–Sivashinsky equation: The Kuramoto-Sivashinsky (KS) equation, originally developed to model the unstable behavior of flame fronts (Kuramoto, 1978), models a chaotic one-dimensional system $\dot{u}(t) = -\frac{\partial^2 u}{\partial x^2} - \frac{\partial^4 u}{\partial x^4} - u \cdot \nabla u$. We consider a one-parameter inverse problem:

$$\dot{u}(t) = \alpha \cdot G(x) - \frac{\partial^2 u}{\partial x^2} - \frac{\partial^4 u}{\partial x^4} - \beta \cdot u \cdot \nabla u.$$

where $G(x)$ is a fixed time-independent forcing term; $\alpha, \beta \in \mathbb{R}$ are the unknown parameters governing the evolution. Each inverse problem starts from a randomly generated initial state $u(t=0)$ and is simulated until $t = 75$, at which point the system becomes chaotic but is still smooth enough to allow for gradient-based optimization. We constrain $\alpha \in [-1, 1]$, $\beta \in [\frac{1}{4}, \frac{3}{4}]$ for numerical stability.

Billiards Setup: Unlike the first two problems which are unidimensional, we also evaluate the performance of the proposed methodology on 2D and 4D classical billiards setup inspired by previous works (Hu et al., 2020). In the two-dimensional Billiards problem, the angle of strike (α) and initial vertical coordinate of the cue ball (y_{cue}^0) are treated as target control parameters. We add initial horizontal coordinate (x_{cue}^0) and the speed of the cue ball as additional target control parameters for the four-dimensional problem. The initial location of all the balls (except for the cue ball) is fixed to ensure a fixed initial state (Y_0) for all the possible trajectories. For effective utilization of computational resources, we extract *key states* and *key times* based on collision occurrences which are subsequently used to generate a linear trajectory. For a given linear trajectory of states or a subset, the goal is to predict the true angle of strike (α^*) and the initial vertical position of the cue ball (y_0^*). The temporal evolution of the billiards’ trajectory, Y^* , encodes the underlying physical laws that govern the collisions and motion of the balls.

It is important to note that the loss landscapes for the billiards system and the Kuramoto-Sivashinsky equation are very complex (See Figure 2) with several occurrences of local minima, flat regions, and sharp gradients that are susceptible to slow convergence or convergence to local minima using BFGS.

3.2 Model Configurations

Training Data: We leverage forward simulation datasets for each discussed non-linear physical system. Training the networks with numerically simulated trajectories offers several advantages. Firstly, numerical solutions from the forward solution of PDEs incorporate physical constraints into the system evolution. Secondly, it overcomes the challenges associated with experimental data, which is costly to obtain and often affected by external noise. Lastly, these ProxyNNs can be trained on arbitrarily large amounts of simulation data by solving the underlying PDEs.

We augment the network inputs $[Y^*, X_s]$ with Fourier features (\mathcal{F}) which have been shown to reduce spectral bias in Tancik et al. (2020). For example, in each training step in the billiards setup, the network is given access to the full (or a subset) trajectory as one of the inputs $\mathcal{F}(Y^*)$ along with unrelated control parameters $\mathcal{F}(X_s) = \{\alpha_s, y_{s,cue}^0\}$ for 2D and $\mathcal{F}(X_s) = \{y_{s,cue}^0, x_{s,cue}^0, \alpha_s, v_{cue}^0\}$ for the 4-D inverse problem to predict the corresponding configuration loss. For 1-D physical systems, we only sample one to two random control parameters for a given starting state (see Table 1) as ProxyNNs are able to generalize even with low-sampling values. Whereas, for Billiards, since there is only one unique starting state, we always sample the target control parameters.

Hyperparameters: We set the learning rate to 0.001. The batch size, and the number of epochs vary according to the system complexity (see Appendix A). Simulation hyperparameters such as the time step for the Burgers' equation and Kuramoto-Shivashinsky equation ($T = 0.5$), coefficient of friction ($\mu = 0.5$), and elasticity ($e = 0.8$) for the billiards setup were fixed apriori. We trained multiple ProxyNNs with varying hyperparameters $\{\sigma, \mu\}$ to empirically investigate the effect of regularization on the complexity of deep neural networks. A summarize the network configurations and all the hyperparameters for the ProxyNNs for different physical systems. All experiments were conducted on a single Nvidia GTX 1080 Ti using PhiFlow (Holl et al., 2020).¹ Training and optimization for each problem takes a maximum of 6-8 hours.

Baselines: We compare our two-step optimization approach using ProxyNN with BFGS and Gradient Descent (GD) on the ground truth loss landscapes.

3.3 Optimization Performance Evaluation

For each physical system discussed in (§ 3.1), we predict the inverse solution, X_p , using the optimization scheme discussed in (§ 2.4) on the regularized ProxyNNs. For estimating the convergence accuracy, we evaluate the prediction error (e) and the re-simulation error (r) as:

$$e = |X_p - X^*| \quad (5)$$

$$r = \|\mathcal{P}(Y_0, X_p) - \mathcal{P}(Y_0, X^*)\|_2^2 \quad (6)$$

where X^* and X_p^* are the true and predicted values of the control parameters, respectively. The re-simulation error measures the L2 distance between the trajectories originating from the same initial state, Y_0 and using the predicted and true values of control parameters.

We further report the convergence accuracy for the top-performing regularized proxy network for all inverse setups discussed in (§ 3.1) for a range of prediction error thresholds, given by:

$$\text{Accuracy} = \frac{\text{Number of predictions with } e \leq \text{threshold}}{\text{Total number of predictions}} \times 100 \quad (7)$$

4 Results

In this section, we show that ProxyNNs successfully predict and approximate configuration loss landscapes, \mathcal{L} , for each of the physical systems discussed in section 3.1. Further, we find that the underlying complexity of these networks can be modulated using regularization techniques (§ 2.3), which subsequently enhances the optimization performance (§ 2.4).

Proxy Neural Networks Predict Loss Landscapes Figure 3 shows that the unregularized ProxyNNs recovers the corresponding *configuration loss* \mathcal{L} for all the inverse problems tested. Although, the ground truth configuration loss function is trivial to optimize in the Burgers equation using

¹<https://github.com/tum-pbs/PhiFlow>

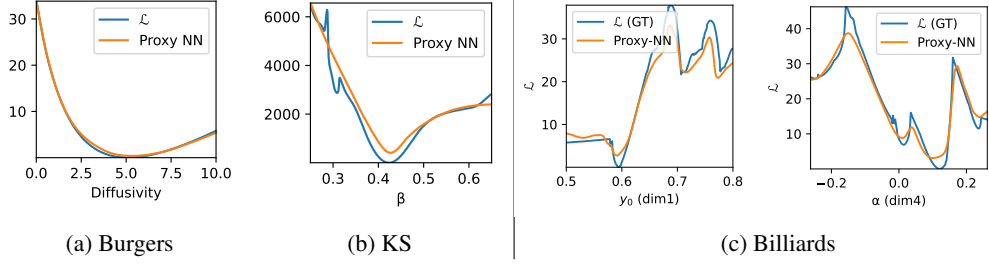


Figure 3: ProxyNNs predict configuration loss landscapes \mathcal{L} .

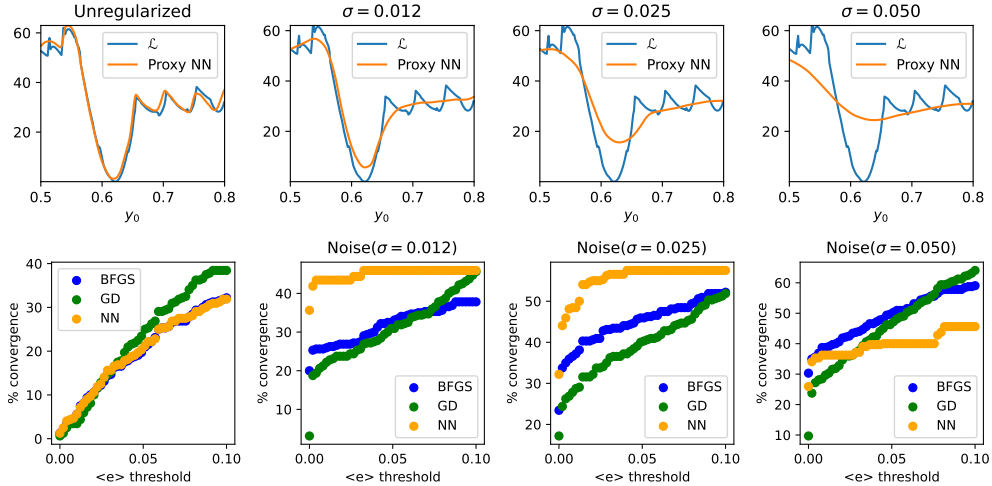


Figure 4: Predicted Loss Landscapes (top) and Optimization performance (bottom) of ProxyNNs in the Billiards setup trained with various regularization hyperparameter $\sigma = \{0, 0.050\}$.

BFGS, it acts as a crucial validation that underscores the capabilities of deep networks to predict and approximate the configuration loss landscape governed by non-linear PDEs.

Unlike the Burgers equation, the configuration loss landscape for the billiards setup and the Kuramoto-Shivashinsky equation is non-trivial with frequent occurrences of local minima, and sharp or vanishing gradients in the target landscape. Figure 3(c) shows the ProxyNN predicted landscape for the 4-dimensional billiards setup along y_{cue}^0 initial location of the cue ball (true value: $y_{cue}^* = 0.59$) and the angle of strike (true value: $\alpha^* = 0.134$). We show the other dimensions for the 4D Billiards setup in Appendix Figure 8. ProxyNNs effectively capture most geometric features of the loss landscape and include essential information about the true parameters at the global minimum. However, addressing the optimization challenges outlined in section 1 remains imperative. This is where the potential to control and regulate the complexity of ProxyNNs presents an opportunity.

Regularization Reduces Complexity In Section 2.3, we propose to regulate the complexity of the loss landscape predicted by ProxyNN using regularization methods. We show the impact of varying the hyperparameter, $\sigma = \{0.0, 0.0125, 0.025, 0.050\}$, on the predicted loss landscape (first row) and convergence accuracy (second row) for the billiards setup (control parameter is the initial position of cue ball y_0), in Figure 4. As σ increases, the learned loss landscape gets increasingly smoother around the global minimum. Unlike the “Unregularized” ProxyNN, which yields the same convergence accuracy as BFGS, regularized ProxyNNs consistently improve convergence accuracy over baselines (BFGS and GD). However, for high sigma values $\sigma = 0.05$, the network produces “too simplified” loss curve, which again yields poor convergence. This demonstrates that the regularization strength plays a key role in simplifying the ProxyNN’s complexity and can improve convergence accuracy if controlled properly.

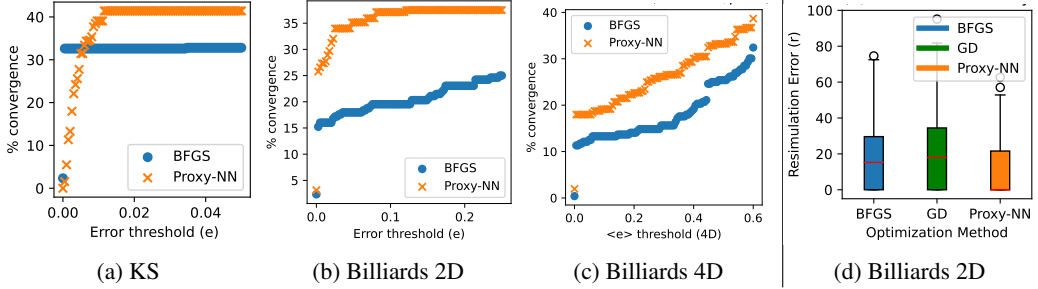


Figure 5: For 256 unique inverse problems for each setup, we report convergence accuracy with varying error thresholds: Regularized ProxyNN results in improved accuracy across the board.

Regularized ProxyNNs Improve Convergence ProxyNN consistently yields better convergence across various error thresholds as shown in Figure 5. We also observe that the convergence to the optimal solution almost doubles when using BFGS on ProxyNN predicted loss compared to ground truth loss in the 2-D billiards setup. Furthermore, the resimulation error is low for ProxyNN compared to other methods. For the Kuramoto–Sivashinsky problem, we can observe that BFGS yields a consistent accuracy score across error thresholds. We find that this is because BFGS either converges on some problems or it does not as shown in Figure 6, whereas ProxyNN results in closer approximation to real β values across the board.

The improvement in convergence accuracy using ProxyNN can be attributed to the smoothening of the loss via the regularization method and the two-step optimization process. The primary optimization step on the regularized ProxyNNs effectively side-steps the local minima, sharp gradients, and flat regions due to underlying regularization. Additionally, the secondary optimization step further enhances the convergence accuracy through the necessary course correction once the vicinity of the global minimum, i.e., the region of interest, is attained.

5 Related Work

In recent years, the exploration of machine learning-based methods, including Deep Neural Networks (DNNs) (Genzel et al., 2020; Chouzenoux et al., 2021; Cao et al., 2022; Antil et al., 2023; Long & Zhe, 2024), Generative Adversarial Networks (GANs), Variational Autoencoders (VAE), and Bayesian Neural Networks (BNNs), has gained prominence for their potential applications in approximating complex partial differential equations (PDEs) in both forward (Pfrommer et al., 2018; Nabian & Meidani, 2018; Michoski et al., 2020; Anantha Padmanabha & Zabaras, 2021; Shen et al., 2022) and inverse problems (Anirudh et al., 2018; Sahli Costabal et al., 2020; Ray, 2021; Zhao et al., 2022; Wu et al., 2022; Jagtap et al., 2022). Physics-informed neural networks (PINNs) have also emerged as effective tools, integrating established physical laws and constraints into their architecture and training procedures, thereby leveraging prior knowledge of underlying physics to guide the learning process (Raissi et al., 2019; Cai et al., 2021; Mao et al., 2020; Zhi et al., 2023; Li et al., 2023; Oommen & Srinivasan, 2022; Fan et al., 2020; Dittmer et al., 2020; Afkham et al., 2021; Ren et al., 2023). Furthermore, studies have underscored the success of training deep networks using data generated by numerical solvers (Guo et al., 2016; Dias Ribeiro et al., 2020; Wolf et al., 2020).

Ren et al. (2021) highlighted that by using DNNs as surrogates for the forward model, it is possible to search for good inverse solutions by implementing backpropagation concerning the model inputs. Further, in variations of this approach, termed Neural Adjoint (NA), it has been shown that adding a boundary loss term improves the performance of this method. In the realm of other effective optimization techniques, Bayesian optimization (Shahriari et al., 2015; Snoek et al., 2012a,b) is one such promising alternative that provides a robust probabilistic framework for addressing non-linear

inverse problems by iteratively exploring and updating the parameter space using observed data. Despite its effectiveness, the method incurs a significant computational cost, primarily attributed to the repeated evaluations of the forward model for each parameter set. Moreover, the efficiency of Bayesian optimization tends to diminish rapidly in high-dimensional inverse loss landscapes. Unlike these approaches, our work aims at directly modeling and using the configuration loss landscapes to identify global minima. By controlling the complexity of the loss landscapes using various regularization methods during training, we identify regions of interest for potential solutions.

6 Limitations and Future Work

As emphasized, the influence of regularization on the learning mechanism of the proxy network relies on the inherent non-linearity of the underlying partial differential equation (PDE). This calls for additional exploration to unveil the empirical correlation between the regularization hyperparameters and the geometric complexity of the network. Such an inquiry can be instrumental in fine-tuning and identifying optimal hyperparameters to achieve the desired predictive capabilities.

Furthermore, while we indeed consider complex 2D and 4D problems, the application of our approach to even more complicated and challenging higher-dimensional problems remains uninvestigated. It would also be interesting to study whether the same underlying network can learn to understand and solve multiple inverse problems together in a multi-task fashion and whether there is any benefit of sharing information across problems. Using neural networks to simulate forward problems is another dimension we do not fully explore as our goal was to focus on modeling the loss landscape induced by the inverse problems.

7 Conclusion

The framework introduced for generalized configuration loss in this study applies to a range of inverse problems where the system trajectory is observable, and the goal is to identify the inverse parameters that influence the trajectory. Neural networks exhibit significant potential in indirectly predicting intricate loss relations between system observables and randomly sampled target parameters. Additionally, ProxyNNs trained with Fourier feature mappings, showcase effective utilization of model capacity, faster convergence, and enhanced sensitivity to the regularization methods.

Additionally, we explore how the learning dynamics of ProxyNNs can be shaped using regularization methods, introducing a regularization pressure aimed at managing the inherent complexity. This ability to control complexity positions solutions based on ProxyNNs as effective choices for addressing inverse problems. We observe that the regularization methods discussed in section 2.3 consistently simplify the geometrically intricate features of the underlying loss landscape, allowing for fine-tuning through corresponding hyperparameters.

The observed optimization performance of BFGS on the regularized ProxyNNs in section 4 provides empirical support that the learning dynamics of neural networks can be harnessed to exert control over their inherent complexity. This, in turn, proves beneficial for the optimization process within existing iterative optimizers, enabling them to predict optimal parameters more effectively.

References

- Afkham, B. M., Chung, J., and Chung, M. Learning regularization parameters of inverse problems via deep neural networks. *Inverse Problems*, 37(10):105017, 2021.
- Anantha Padmanabha, G. and Zabaras, N. Solving inverse problems using conditional invertible neural networks. *Journal of Computational Physics*, 433:110194, 2021. ISSN 0021-9991. doi: <https://doi.org/10.1016/j.jcp.2021.110194>. URL <https://www.sciencedirect.com/science/article/pii/S0021999121000899>.
- Anirudh, R., Thiagarajan, J. J., Kailkhura, B., and Bremer, T. An unsupervised approach to solving inverse problems using generative adversarial networks. *arXiv preprint arXiv:1805.07281*, 2018.
- Antil, H., Elman, H. C., Onwunta, A., and Verma, D. A deep neural network approach for parameterized pdes and bayesian inverse problems. *Machine Learning: Science and Technology*, 4

(3):035015, aug 2023. doi: 10.1088/2632-2153/ace67c. URL <https://dx.doi.org/10.1088/2632-2153/ace67c>.

Blanc, G., Gupta, N., Valiant, G., and Valiant, P. Implicit regularization for deep neural networks driven by an ornstein-uhlenbeck like process, 2020.

Broyden, C., Fletcher, R., Goldfarb, D., and Shanno, D. Convergence properties of a class of quasi-newton methods in optimization. *Journal of Mathematical Programming*, 6(2):163–175, 1970.

Buhrmester, V., Münch, D., and Arens, M. Analysis of explainers of black box deep neural networks for computer vision: A survey. *Machine Learning and Knowledge Extraction*, 3(4):966–989, 2021. ISSN 2504-4990. doi: 10.3390/make3040048. URL <https://www.mdpi.com/2504-4990/3/4/48>.

Burgers, J. M. A mathematical model illustrating the theory of turbulence. *Advances in applied mechanics*, 1:171–199, 1948.

Cai, S., Wang, Z., Wang, S., Perdikaris, P., and Karniadakis, G. E. Physics-Informed Neural Networks for Heat Transfer Problems. *Journal of Heat Transfer*, 143(6), 04 2021. ISSN 0022-1481. doi: 10.1115/1.4050542. URL <https://doi.org/10.1115/1.4050542>. 060801.

Cao, N., Xie, J., Zhang, A., Hou, S.-Y., Zhang, L., and Zeng, B. Neural networks for quantum inverse problems. *New Journal of Physics*, 24(6):063002, June 2022. doi: 10.1088/1367-2630/ac706c.

Chouzenoux, E., Della Valle, C., and Pesquet, J.-C. Inversion of Integral Models: a Neural Network Approach. *arXiv e-prints*, art. arXiv:2105.15044, May 2021. doi: 10.48550/arXiv.2105.15044.

Dherin, B., Munn, M., Rosca, M., and Barrett, D. G. T. Why neural networks find simple solutions: the many regularizers of geometric complexity, 2022.

Dias Ribeiro, M., Rehman, A., Ahmed, S., and Dengel, A. DeepCFD: Efficient Steady-State Laminar Flow Approximation with Deep Convolutional Neural Networks. *arXiv e-prints*, art. arXiv:2004.08826, April 2020. doi: 10.48550/arXiv.2004.08826.

Dittmer, S., Kluth, T., Maass, P., and Otero Baguer, D. Regularization by architecture: A deep prior approach for inverse problems. *Journal of Mathematical Imaging and Vision*, 62:456–470, 2020.

Fan, T., Xu, K., Pathak, J., and Darve, E. Solving inverse problems in steady-state navier-stokes equations using deep neural networks, 2020.

Fung, V., Zhang, J., Hu, G., Ganesh, P., and Sumpter, B. G. Inverse design of two-dimensional materials with invertible neural networks. *npj Computational Materials*, 7(1):200, Dec 2021. ISSN 2057-3960. doi: 10.1038/s41524-021-00670-x. URL <https://doi.org/10.1038/s41524-021-00670-x>.

Genzel, M., Macdonald, J., and März, M. Solving Inverse Problems With Deep Neural Networks – Robustness Included? *arXiv e-prints*, art. arXiv:2011.04268, November 2020. doi: 10.48550/arXiv.2011.04268.

Goodfellow, I., Bengio, Y., and Courville, A. *Deep Learning*. MIT Press, 2016. <http://www.deeplearningbook.org>.

Gramacy, R. B. and Lee, H. K. H. Optimization under unknown constraints, 2010.

Guo, X., Li, W., and Iorio, F. Convolutional neural networks for steady flow approximation. In *Proceedings of the 22nd ACM SIGKDD International Conference on Knowledge Discovery and Data Mining*, KDD '16, pp. 481–490, New York, NY, USA, 2016. Association for Computing Machinery. ISBN 9781450342322. doi: 10.1145/2939672.2939738. URL <https://doi.org/10.1145/2939672.2939738>.

Holl, P., Koltun, V., Um, K., and Thuerey, N. phiflow: A differentiable pde solving framework for deep learning via physical simulations. In *NeurIPS workshop*, volume 2, 2020.

Hopf, E. The partial differential equation. 1950.

- Hu, Y., Anderson, L., Li, T.-M., Sun, Q., Carr, N., Ragan-Kelley, J., and Durand, F. Diffitaichi: Differentiable programming for physical simulation, 2020.
- Huang, S., Xiang, J., Du, H., and Cao, X. Inverse problems in atmospheric science and their application. *Journal of Physics: Conference Series*, 12(1):45, jan 2005. doi: 10.1088/1742-6596/12/1/005. URL <https://dx.doi.org/10.1088/1742-6596/12/1/005>.
- Jagtap, A. D., Mao, Z., Adams, N., and Karniadakis, G. E. Physics-informed neural networks for inverse problems in supersonic flows. *Journal of Computational Physics*, 466:111402, oct 2022. doi: 10.1016/j.jcp.2022.111402. URL <https://doi.org/10.1016%2Fj.jcp.2022.111402>.
- Kingma, D. P. and Ba, J. Adam: A method for stochastic optimization, 2017.
- Kuramoto, Y. Diffusion-Induced Chaos in Reaction Systems. *Progress of Theoretical Physics Supplement*, 64:346–367, January 1978. doi: 10.1143/PTPS.64.346.
- Langley, P. Crafting papers on machine learning. In Langley, P. (ed.), *Proceedings of the 17th International Conference on Machine Learning (ICML 2000)*, pp. 1207–1216, Stanford, CA, 2000. Morgan Kaufmann.
- Li, Y., Wang, Y., and Yan, L. Surrogate modeling for bayesian inverse problems based on physics-informed neural networks. *Journal of Computational Physics*, 475:111841, 2023. ISSN 0021-9991. doi: <https://doi.org/10.1016/j.jcp.2022.111841>. URL <https://www.sciencedirect.com/science/article/pii/S0021999122009044>.
- Long, D. and Zhe, S. Invertible fourier neural operators for tackling both forward and inverse problems, 2024.
- Mao, Z., Jagtap, A. D., and Karniadakis, G. E. Physics-informed neural networks for high-speed flows. *Computer Methods in Applied Mechanics and Engineering*, 360:112789, 2020.
- McCann, M. T., Jin, K. H., and Unser, M. Convolutional neural networks for inverse problems in imaging: A review. *IEEE Signal Processing Magazine*, 34(6):85–95, 2017. doi: 10.1109/MSP.2017.2739299.
- Michoski, C., Milosavljević, M., Oliver, T., and Hatch, D. R. Solving differential equations using deep neural networks. *Neurocomputing*, 399:193–212, 2020. ISSN 0925-2312. doi: <https://doi.org/10.1016/j.neucom.2020.02.015>. URL <https://www.sciencedirect.com/science/article/pii/S0925231220301909>.
- Mohammad-Djafari, A. Regularization, bayesian inference, and machine learning methods for inverse problems. *Entropy*, 23(12):1673, 2021.
- Nabian, M. A. and Meidani, H. A deep neural network surrogate for high-dimensional random partial differential equations. *CoRR*, abs/1806.02957, 2018. URL <http://arxiv.org/abs/1806.02957>.
- Oommen, V. and Srinivasan, B. Solving Inverse Heat Transfer Problems Without Surrogate Models: A Fast, Data-Sparse, Physics Informed Neural Network Approach. *Journal of Computing and Information Science in Engineering*, 22(4):041012, 03 2022. ISSN 1530-9827. doi: 10.1115/1.4053800. URL <https://doi.org/10.1115/1.4053800>.
- Oulghelou, M., Beghein, C., and Allery, C. A surrogate optimization approach for inverse problems: Application to turbulent mixed-convection flows. *Computers & Fluids*, 241:105490, 2022. ISSN 0045-7930. doi: <https://doi.org/10.1016/j.compfluid.2022.105490>. URL <https://www.sciencedirect.com/science/article/pii/S0045793022001311>.
- Pfrommer, J., Zimmerling, C., Liu, J., Kärger, L., Henning, F., and Beyerer, J. Optimisation of manufacturing process parameters using deep neural networks as surrogate models. *Procedia CIRP*, 72: 426–431, 2018. ISSN 2212-8271. doi: <https://doi.org/10.1016/j.procir.2018.03.046>. URL <https://www.sciencedirect.com/science/article/pii/S221282711830146X>. 51st CIRP Conference on Manufacturing Systems.

- Raissi, M., Perdikaris, P., and Karniadakis, G. Physics-informed neural networks: A deep learning framework for solving forward and inverse problems involving nonlinear partial differential equations. *Journal of Computational Physics*, 378:686–707, 2019. ISSN 0021-9991. doi: <https://doi.org/10.1016/j.jcp.2018.10.045>. URL <https://www.sciencedirect.com/science/article/pii/S0021999118307125>.
- Ray, D. Solving physics-based inverse problems using gans. 2021.
- Ren, P., Rao, C., Sun, H., and Liu, Y. Physics-informed neural network for seismic wave inversion in layered semi-infinite domain, 2023.
- Ren, S., Padilla, W., and Malof, J. Benchmarking deep inverse models over time, and the neural-adjoint method, 2021.
- Ruder, S. An overview of gradient descent optimization algorithms, 2017.
- Sahli Costabal, F., Yang, Y., Perdikaris, P., Hurtado, D. E., and Kuhl, E. Physics-informed neural networks for cardiac activation mapping. *Frontiers in Physics*, 8:42, 2020.
- Savović, S., Ivanović, M., and Min, R. A comparative study of the explicit finite difference method and physics-informed neural networks for solving the burgers; equation. *Axioms*, 12(10), 2023. ISSN 2075-1680. doi: 10.3390/axioms12100982. URL <https://www.mdpi.com/2075-1680/12/10/982>.
- Shahriari, B., Swersky, K., Wang, Z., Adams, R. P., and De Freitas, N. Taking the human out of the loop: A review of bayesian optimization. *Proceedings of the IEEE*, 104(1):148–175, 2015.
- Shen, L., Li, D., Zha, W., Li, X., and Liu, X. Surrogate modeling for porous flow using deep neural networks. *Journal of Petroleum Science and Engineering*, 213:110460, 2022. ISSN 0920-4105. doi: <https://doi.org/10.1016/j.petrol.2022.110460>. URL <https://www.sciencedirect.com/science/article/pii/S092041052200345X>.
- Snoek, J., Larochelle, H., and Adams, R. P. Practical bayesian optimization of machine learning algorithms. In Pereira, F., Burges, C., Bottou, L., and Weinberger, K. (eds.), *Advances in Neural Information Processing Systems*, volume 25. Curran Associates, Inc., 2012a. URL https://proceedings.neurips.cc/paper_files/paper/2012/file/05311655a15b75fab86956663e1819cd-Paper.pdf.
- Snoek, J., Larochelle, H., and Adams, R. P. Practical bayesian optimization of machine learning algorithms, 2012b.
- Tancik, M., Srinivasan, P. P., Mildenhall, B., Fridovich-Keil, S., Raghavan, N., Singhal, U., Ramamoorthi, R., Barron, J. T., and Ng, R. Fourier features let networks learn high-frequency functions in low dimensional domains. *CoRR*, abs/2006.10739, 2020. URL <https://arxiv.org/abs/2006.10739>.
- Winovich, N., Ramani, K., and Lin, G. Convpdde-uq: Convolutional neural networks with quantified uncertainty for heterogeneous elliptic partial differential equations on varied domains. *Journal of Computational Physics*, 394:263–279, 2019. ISSN 0021-9991. doi: <https://doi.org/10.1016/j.jcp.2019.05.026>. URL <https://www.sciencedirect.com/science/article/pii/S0021999119303572>.
- Wolf, B., Donzallaz, J., Jost, C., Hayoz, A., Commend, S., Hennebert, J., and Kuonen, P. Using cnns to optimize numerical simulations in geotechnical engineering. In *Artificial Neural Networks in Pattern Recognition: 9th IAPR TC3 Workshop, ANNPR 2020, Winterthur, Switzerland, September 2–4, 2020, Proceedings*, pp. 247–256, Berlin, Heidelberg, 2020. Springer-Verlag. ISBN 978-3-030-58308-8. doi: 10.1007/978-3-030-58309-5_20. URL https://doi.org/10.1007/978-3-030-58309-5_20.
- Wu, H., O’Malley, D., Golden, J. K., and Vesselinov, V. V. Inverse analysis with variational autoencoders: A comparison of shallow and deep networks. *Journal of Machine Learning for Modeling and Computing*, 3(2), 2022.

Würth, T., Krauß, C., Zimmerling, C., and Kärger, L. Physics-informed neural networks for data-free surrogate modelling and engineering optimization – an example from composite manufacturing. *Materials & Design*, 231:112034, 2023. ISSN 0264-1275. doi: <https://doi.org/10.1016/j.matdes.2023.112034>. URL <https://www.sciencedirect.com/science/article/pii/S0264127523004495>.

Zhao, Q., Lindell, D. B., and Wetzstein, G. Learning to solve pde-constrained inverse problems with graph networks, 2022.

Zhi, P., Wu, Y., Qi, C., Zhu, T., Wu, X., and Wu, H. Surrogate-based physics-informed neural networks for elliptic partial differential equations. *Mathematics*, 11(12), 2023. ISSN 2227-7390. doi: 10.3390/math11122723. URL <https://www.mdpi.com/2227-7390/11/12/2723>.

A Hyperparameter Configuration

The network hyperparameters for each of the settings and the dataset details are summarized below:

System	# Input Dim	Architecture	# Parameters ($\times 10^3$)	Dataset Size ($\times 10^3$)	Batch Size	Sampling Rate	(σ, μ)
Rastrigin Test function	1	DenseNet [64,128,128,128,64]	49.7	NR	256	NA	([0.20, 0.50], 1)
Gramacy & Lee Test function	1	DenseNet [64,128,256,128,64]	82.7	NR	256	NA	([0.17, 0.27], 20)
Burgers' equation	2	ConvNet [128,128,128]	107.6	32	128	2	NR
Kuramoto-Sivashinsky equation	16	ConvNet with \mathcal{F} [32, 64, 128, 256, 128, 64, 32]	779.5	1280	256	2	({0.005, 0.021, 0.1}, 5)
Billiards-2D Setup	40	ConvNet with \mathcal{F} [32,64,128,256,128,64,32]	740.9	640	128	640k	({0.013, 0.018, 0.025, 0.027, 0.050}, 5)
Billiards-4D Setup	64	ConvNet with \mathcal{F} [32,64,128,256,128,64,32]	740.9	2560	256	2560k	({0.013, 0.018, 0.025, 0.027, 0.050}, 5)

Table 1: Training details for test functions and physical systems. NR = Not Required. In both 2D and 4D Billiards, there is only one unique initial state.

B Optimization policy and results

The two-step optimization strategy and performance are depicted in figure 7. We aim to locate the “region of interest” in the control parameter search space Z that contains the global minimum through the primary optimization step. This effectively narrows down the search limit to the vicinity of the global minimum. Furthermore, starting from the primary convergence point (X_1^*) we achieve convergence close to the global minimum (X_p^*) through final optimization on the ground truth configuration loss, \mathcal{L} .

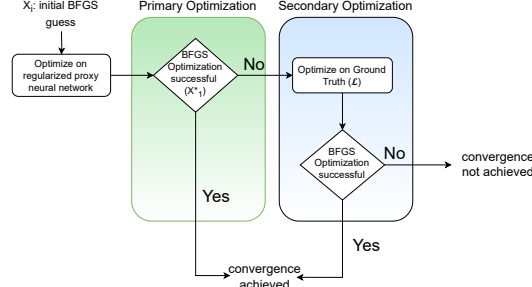


Figure 7: Two-Step optimization policy for ProxyNNs. The primary step aims to converge in the vicinity of the global minimum which is treated as initial guess for the secondary optimization step.

C ProxyNN predicted Configuration Loss landscapes for 4D Billiards

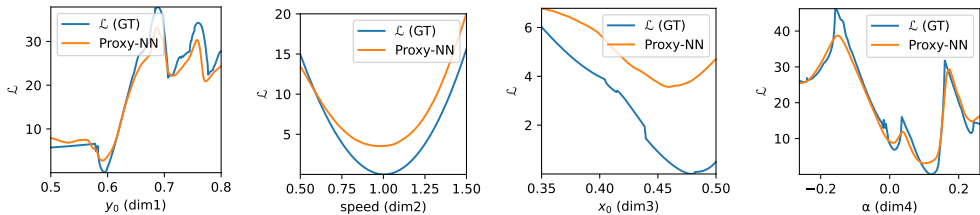


Figure 8: Proxy networks predicts configuration loss landscape \mathcal{L} in the 4-D Billiards Inverse Setup.